Dynamics of Bose-Einstein condensates: Variational solutions of the Gross-Pitaevskii equations

Víctor M. Pérez-García
Departamento de Matemáticas, Escuela Técnica Superior de Ingenieros Industriales, Universidad de Castilla-La Mancha, 13071 Ciudad Real, Spain

Humberto Michinel
Departamento de Ingenieria Mecánica, Naval y Oceánica Escuela Politécnica Superior, Universidade de A Coruña, 15706 Ferrol, Spain

J. I. Cirac
Institute for Theoretical Physics, University of Innsbruck, A–6020 Innsbruck, Austria

M. Lewenstein
Comissariat a l'Energie Atomique, DSM/DRECAM/SPAM, Centre d'Etudes de Saclay, 91191 Gif-sur-Yvette, France

P. Zoller
Institute for Theoretical Physics, University of Innsbruck, A–6020 Innsbruck, Austria
(Received 14 March 1997)

A variational technique is applied to solve the time-dependent nonlinear Schrödinger equation (Gross-Pitaevskii equation) with the goal to model the dynamics of dilute ultracold atom clouds in the Bose-Einstein condensed phase. We derive analytical predictions for the collapse, equilibrium widths, and evolution laws of the condensate parameters and find them to be in very good agreement with our numerical simulations of the nonlinear Schrödinger equation. It is found that not only the number of particles, but also both the initial width of the condensate and the effect of different perturbations to the condensate may play a crucial role in the collapse dynamics. The results are applicable when the shape of the condensate is sufficiently simple. [S1050-2947(97)04408-9]

PACS number(s): 03.75.Fi

I. INTRODUCTION

It has been more than 70 years since the prediction of Bose [1] and Einstein [2] that a system of noninteracting bosons would undergo a phase transition to a state having a macroscopic population of the ground state at finite (low) temperature. However, it has only been very recently that laser cooling and evaporative cooling techniques [3,4], combined with development of novel traps, led to first unambiguous observations of Bose-Einstein condensation of a weakly interacting atomic Bose gas in the laboratory [5–8].

On the theory side, the dynamics of dilute trapped Bose-Einstein gases has been successfully modeled by mean-field theories [9]. In particular, it has been shown recently by several groups that the Gross-Pitaevskii equation (GPE), a nonlinear Schrödinger equation (NLSE) for the macroscopic wave function of the Bose-Einstein condensed gas, provides an accurate description of the ground state and of the excitation spectrum of the condensate at (or close to) zero temperature [10–18]. Most of the theoretical work to solve the Gross-Pitaevskii equation has focused on the Thomas-Fermi limit, which corresponds to the case where the nonlinear interaction term in the GPE (the atomic interaction term) is much larger than the bare trap excitation energies, i.e., the limit of large particle numbers [11,12]. On the other hand, numerical studies of equilibrium conditions and excitation spectra were performed solving the GPE for a wide range of parameters from the limit of small to large particle numbers and found to be in excellent agreement with experiment [10,15]. In recent work we have proposed a variational technique that allows one to obtain essentially analytical solutions of the GPE. In particular, we [18] have proposed a variational technique that allows one to describe the dynamics of the condensate as a function of a few parameters (width of the cloud, center, etc.), which in turn satisfy very simple equations. In this paper we elaborate on these results, and present some predictions concerning the regime in which collapse takes place for negative scattering lengths. These predictions can be tested with current experimental setups [7].

Let us consider a boson gas with a fixed mean number of particles N, moving in a potential well that represents the trap. If the particle density and temperature of the condensate are sufficiently small, the dynamics of the Bose-Einstein condensed atoms is described by the NLSE (or GPE) [19]

$$i\hbar \frac{\partial \psi}{\partial t} = -\frac{\hbar^2}{2m}\nabla^2\psi + V(r)\psi + U_0|\psi|^2\psi, \tag{1}$$

where $U_0 = 4\pi\hbar^2 a/m$ characterizes the interaction and is defined in terms of the ground-state scattering length a. The normalization for ψ is $N = \int |\psi|^2 d^3\vec{r}$. The potential can be taken as

$$V(\vec{r})=\frac{1}{2}m\nu^2(\lambda_x^2x^2+\lambda_y^2y^2+\lambda_z^2z^2), \tag{2}$$

$\lambda_\eta(\eta=x,y,z)$ being constants describing the anisotropies of the trap [20]. In present experimental situations we have $\lambda_x=\lambda_y=1$ and $\lambda_z=\nu_z/\nu$, which denotes the ratio of the frequency along the z direction ν_z to the radial frequency $\nu_r\equiv\nu$.

The NLSE is is a nonlinear equation well known in mathematical physics [21]. In particular, the three-dimensional NLSE is a universal equation, which appears in various problems in many branches of physics, such as fiber and integrated optics, when investigating paraxial propagation of laser beams in nonlinear optical waveguides. In the past, (1+1)- and (2+1)-dimensional cases have been studied by many authors using different approaches, including variational techniques [22,23], moment theory [24], soliton perturbation methods [25], and, of course, numerical methods [26,27].

In three-dimensional problems numerical simulations are expensive. This is why it is very important to be able to give analytical information on the solutions, which complement the numerical studies. In these three-dimensional problems the only analytical tool available up to now to avoid the numerical simulations is the variational technique [22,23]. This technique is based on Ritz's optimization procedure and has been widely used when studying the NLS equations that appear in nonlinear optics [28], but also in many other physical problems where nonlinear wave equations arise [29,30]. Although not exact, this technique is a good method to study the propagation of distributions having simple shape and in many cases provides not only qualitative but quantitative results. The basic idea of the variational method is to take a trial function with a fixed shape but some free parameters in order to reduce the infinite-dimensional problem of the partial differential equation to a Newton-like second-order ordinary differential equation for the (variational) parameters that characterize the solution. In other cases, however, the validity of the variational results is only qualitative [31]; i.e., if the shape of the actual solution is close to the trial function, the results obtained with the variational method will be in good agreement with the real solutions, but in other cases the method can be very rough or even fail.

In this paper we will study the application of the variational technique to Eq. (1), which arises in Bose-Einstein condensation problems. This paper is organized as follows: in Sec. II we derive the equations for the evolution of the condensate parameters; in Sec. III we present an analysis of the spherically symmetric case, and make some precise predictions regarding the collapse conditions for negative scattering length. In contrast to other analysis [12], we find that not only is the number of particles present in the condensate important to predict the collapse, but also the initial conditions of the cloud. In Sec. IV, we study the nonsymmetric case and predict existence of compact stable solutions, even when trapping in one direction is eliminated. Finally, in Sec. V, we summarize our conclusions.

II. DERIVATION OF THE EQUATIONS FOR THE VARIATIONAL PARAMETERS

A. Statement of the problem

Let us restate the problem of solving Eq. (1) as a variational problem, corresponding to a stationary point of the action related to the Lagrangian density $\mathcal{L}$:

$$\mathcal{L}=\frac{i}{2}\hbar\left(\psi\frac{\partial\psi^*}{\partial t}-\psi^*\frac{\partial\psi}{\partial t}\right)-\frac{\hbar^2}{2m}|\nabla\psi|^2+V(r)|\psi|^2+\frac{2\pi a\hbar^2}{m}|\psi|^4, \tag{3}$$

where the asterisk denotes complex conjugation. That is, one has to find ψ, such that the action

$$S=\int\mathcal{L}d^3\vec{r}dt \tag{4}$$

is extreme. However, this problem is as complicated as solving the original NLSE. Therefore, to obtain the evolution of the condensate we will find the extremum of Eq. (3) within a set of trial functions. The selection of the proper form of the trial functions is very important. In our case a natural choice is a Gaussian, since in the linear limit we get the ground-state solution of the linear Schrödinger equation in a parabolic potential. Another possible choice is a sech function [32], since in the one-dimensional case one gets the exact soliton solution (nonlinear solution), but this ansatz fails to reproduce the linear limit ,and does not take into account the effect of the potential. So we will choose a Gaussian ansatz of the form

$$\psi(x,y,z,t)=A(t)\prod_{\eta=x,y,z}e^{-[\eta-\eta_0(t)]^2/2w_\eta^2+i\eta\alpha_\eta(t)+i\eta^2\beta_\eta(t)}. \tag{5}$$

For a given value of t, the previous function defines a Gaussian distribution centered at (x_0,y_0,z_0) and described by the parameters A (complex amplitude), w_η (width), α_η (slope), and β_η (curvature radius)$^{-1/2}$. The consideration of the phase term is essential if we want to obtain reliable results, as was shown in related works in nonlinear optics [32]. Concerning what is known about the shape of the condensate wave function, a Gaussian is probably a very reasonable ansatz for the negative scattering length case. In the positive scattering length case, a better shape could be—at least in the strongly nonlinear limit—similar to the Thomas-Fermi solution; however, it is always possible to obtain good fits of these functions by Gaussians.

Our goal is to find the equations governing the evolution of the previous quantities. So, inserting Eq. (5) into Eq. (3) it is possible to calculate an effective Lagrangian by averaging the Lagrangian density, $L=\langle\mathcal{L}\rangle$ as

$$L=\langle\mathcal{L}\rangle=\int_{-\infty}^{+\infty}L\,d^3\vec{r}=\frac{\pi^{3/2}}{2}w_xw_yw_z\Bigg\{i\hbar(A^*\dot{A}-A\dot{A}^*)+|A|^2\sum_{\eta=x,y,z}\Bigg[\left(\dot{\beta}_\eta-\frac{2\hbar^2}{m}\beta_\eta^2-\frac{1}{2}m\nu^2\lambda_\eta^2\right)(w_\eta^2+2\eta_0^2)-\frac{\hbar^2w_\eta^2}{2m}+\frac{\hbar^2\alpha_\eta^2}{m}+2\eta_0\left(\dot{\alpha}_\eta-\frac{2\hbar^2}{m}\alpha_\eta\beta_\eta\right)\Bigg]+\frac{\sqrt{2}\pi\hbar^2a}{m}|A|^4\Bigg\}. \tag{6}$$

The dots denote derivatives with respect to t. At this point, we have reduced the infinite-dimensional problem of solving Eq. (1), or equivalently finding the stationary point of the action corresponding to the Lagrangian density (3), to a finite dimensional problem, i.e., solving the Lagrange equations

$$\frac{d}{dt}\left(\frac{\partial L}{\partial\dot{q}_j}\right)-\frac{\partial L}{\partial q_j}=0. \tag{7}$$

Here, we have used the notation

$$q_j\equiv\{w_x,w_y,w_z,A,A^*,x_0,y_0,z_0,\alpha_x,\alpha_y,\alpha_z,\beta_x,\beta_y,\beta_z\}.$$

The derivation of the evolution equations for the parameters is a straightforward although tedious task. The difficulty increases with the number of parameters and this is why choosing a good small set of parameters is important. Detailed examples of these calculations can be found elsewhere [23,28].

B. Evolution equations for the variational parameters

Let us now discuss the evolution equations for the variational parameters. First, conservation of the number of particles leads to

$$\pi^{3/2}|A(t)|^2w_x(t)w_y(t)w_z(t)=\text{const}=\pi^{3/2}|A(0)|^2w_x(0)w_y(0)w_z(0)=N, \tag{8}$$

Furthermore, the equations for the motion of the center of the condensate are

$$\ddot{\eta}_0+\lambda_\eta^2\nu^2\eta_0=0, \tag{9}$$

with $\eta=x,y,z$. This equation corresponds to a harmonic oscillation of the condensate center with the bare frequencies $\lambda_\eta\nu$. It is interesting and intuitively clear that this motion does not depend on the number of particles N. Thus, the motion of the center of gravity of the cloud will not be affected by the nonlinear effects and depends only on external potentials. This fact is interesting since it implies that the condensate in the mean responds like a classical particle to external effects. On the other hand this is a consequence of the generalized Ehrenfest theorem for the NLS, not a particular result of our approximate approach.

The widths of the condensate satisfy the following equations

$$\ddot{w}_x+\lambda_x^2\nu^2w_x=\frac{\hbar^2}{m^2w_x^3}+\sqrt{\frac{2}{\pi}}\frac{a\hbar^2N}{m^2w_x^2w_yw_z}, \tag{10a}$$

$$\ddot{w}_y+\lambda_y^2\nu^2w_y=\frac{\hbar^2}{m^2w_y^3}+\sqrt{\frac{2}{\pi}}\frac{a\hbar^2N}{m^2w_y^2w_xw_z}, \tag{10b}$$

$$\ddot{w}_z+\lambda_z^2\nu^2w_z=\frac{\hbar^2}{m^2w_z^3}+\sqrt{\frac{2}{\pi}}\frac{a\hbar^2N}{m^2w_z^2w_yw_x}, \tag{10c}$$

which we will analyze in more detail later. The rest of the parameters can be obtained from the widths and center coordinates using the equations

$$\beta_\eta=-\frac{m\dot{w}_\eta}{2\hbar^2w_\eta}, \tag{11a}$$

$$\alpha_\eta=-\frac{m\dot{\eta}_0}{\hbar^2}-2\beta_\eta\eta_0, \tag{11b}$$

with $\eta=x,y,z$. This means that, once we know the center of the condensate and widths, we can calculate the evolution of the rest of the parameters and then completely characterize the evolution of a Gaussian-like atom cloud.

It is convenient to introduce new variables and constants according to $\tau=\nu t,\omega_\eta=a_0v_\eta(\eta=x,y,z)$, and $P=\sqrt{2/\pi}Na/a_0$ where $a_0=\sqrt{\hbar/(m\nu)}$ is the size of the ground state for a harmonic potential of frequency ν (up to a factor $\sqrt{2}$). Note that P basically gives the strength of the atom-atom interactions related to the bare harmonic potential. The case when this parameter is very large corresponds to the Thomas-Fermi limit. Then, the equations for the rescaled widths are

$$\frac{d^2}{d\tau^2}v_x+\lambda_x^2v_x=\frac{1}{v_x^3}+\frac{P}{v_x^2v_yv_z}, \tag{12a}$$

$$\frac{d^2}{d\tau^2}v_y+\lambda_y^2v_y=\frac{1}{v_y^3}+\frac{P}{v_y^2v_xv_z}, \tag{12b}$$

$$\frac{d^2}{d\tau^2}v_z+\lambda_z^2v_z=\frac{1}{v_z^3}+\frac{P}{v_z^2v_xv_y}. \tag{12c}$$

Equations (12a)–(12c) give us a simple picture of the evolution of the width of the condensate because they correspond to the motion of a particle with coordinates (v_x,v_y,v_z) in the classical, three-dimensional potential

$$V(v_x,v_y,v_z)=\frac{1}{2}(\lambda_x^2v_x^2+\lambda_y^2v_y^2+\lambda_z^2v_z^2)+\frac{1}{2v_x^2}+\frac{1}{2v_y^2}+\frac{1}{2v_z^2}+\frac{P}{v_xv_yv_z}. \tag{13}$$

It follows from (12a)–(12c) that the dispersive term, which is proportional to $v_\eta^{-3}(\eta=x,y,z)$, tends to spread the wave-packet. On the other hand, there is one attractive term which

is the linear one and is caused by the trap. Finally, we have the last term which comes from the nonlinear interaction between the particles. Depending on the sign of the scattering length a, which is the same as that of P, this term can be either repulsive (positive scattering length) or attractive (negative scattering length).

Since the center of mass motion is very simple, to understand the condensate dynamics we have to concentrate in the study of Eqs. (12a)–(12c). These are a set of three coupled nonlinear ordinary differential equations. Although the complexity relative to the original problem (1) has been greatly reduced, it is still a complex problem and nonintegrable, since the only conserved quantity is the Hamiltonian. In fact, numerical simulations of Eq. (12) show chaotic oscillations in various cases. It is doubtful, however, that the Gaussian ansatz will be a good solution in those cases, and one would expect that different spatiotemporal complex phenomena appear.

III. ANALYSIS OF THE SPHERICALLY SYMMETRIC CASE

A. Discussion

Let us first concentrate on the homogeneous case, when the trapping potential is spherically symmetric ($\lambda_x=\lambda_y=\lambda_z\equiv 1$). In addition, we will assume that all the widths are equal (radial symmetry case) ($v_x=v_y=v_z=v$), and that initially the condensate is ''at rest'' ($\dot{v}=0$).

Equations (12a)–(12c) reduce to

$$\frac{d^2v}{d\tau^2}+v=\frac{1}{v^3}+\frac{P}{v^4}. \tag{14}$$

This equation can be formally integrated using energy conservation, since

$$E=\frac{1}{2}\left(\frac{dv}{d\tau}\right)^2+\frac{1}{2}v^2+\frac{1}{2v^2}+\frac{P}{3v^3}, \tag{15}$$

so that

$$\tau=\int_{v_0}^{v}\frac{dv'}{\sqrt{2\left[E-\frac{1}{2}v'^2-1/(2v'^2)-P/(3v'^3)\right]}}. \tag{16}$$

However, this formal solution gives little insight into what is happening. The analysis of the equilibrium points v_0 of Eq. (14), which satisfy

$$v_0=\frac{1}{v_0^3}+\frac{P}{v_0^4}, \tag{17}$$

is much more illuminating.

One can easily solve Eq. (17) numerically, and find the oscillation frequencies

$$\nu_a=2\nu\sqrt{1-2P'}, \tag{18a}$$

$$\nu_{b,c}=2\nu[1-P'/2\pm\sqrt{P'^2/4-2P'}]^{1/2}, \tag{18b}$$

where we have defined $P'=P/(4v_0^5)$.

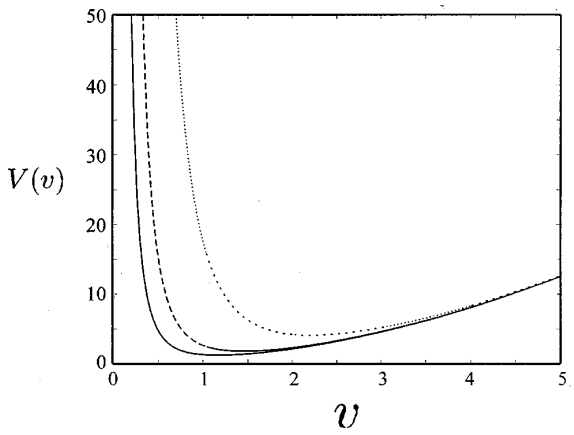

FIG. 1. Potential $V(v)$ for $P=1$ (solid), $P=5$ (dashed), $P=50$ (dotted).

B. Positive scattering length

When $P>0$ Eq. (17) can be rewritten in polynomial form as

$$v_0^5=v_0+P. \tag{19}$$

This is a fifth-order algebraic polynomial problem that has only one positive real root. This solution corresponds to a stable equilibrium point. The potential has a simple shape as can be seen in Fig. 1 where it is plotted for different values of P. It is clear that the only possible motions are periodic (anharmonic) oscillations around the bottom of the ''potential well'' $V(v)$. The frequencies obtained by numerically finding the roots of Eq. (19) and using Eq. (18) agree well with numerical simulations of the NLSE [33].

Equation (19) can be easily analyzed in several regimes. For example, when the interactions are strong $P\gg 1$, one can neglect the term v_0 and obtain $v_0=P^{1/5}$. This corresponds to the Thomas-Fermi regime analyzed by other authors [11]. After linearizing Eq. (14) around the equilibrium position, we find that the oscillation frequencies are $\sqrt{2},\sqrt{5}$, where the first one is doubly degenerate.

C. Negative scattering length

In this case, which corresponds to an attractive nonlinearity, the picture is quite different. Now Eq. (17) can have either no or two positive real solutions. The limiting case (only one solution exists) is given by the equations

$$v_0=\frac{1}{v_0^3}-\frac{|P|}{v_0^4}, \tag{20}$$

$$-\frac{3}{v_0^4}+\frac{4|P|}{v_0^5}=1, \tag{21}$$

which implies that the critical value of P is given by

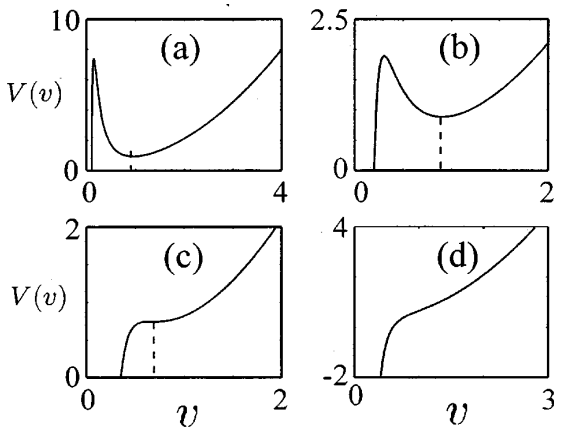

FIG. 2. Potential $V(v)$ for (a) $P=0.15$; (b) $P=0.3$; (c) $P=0.5350$; (d) $P=1$.

$$|P_c| = \frac{4}{5^{5/4}} = 0.5350. \tag{22}$$

In this case we have one metastable equilibrium point. When $P<P_c$, there are no equilibrium points, and all initial data collapse in finite time. In this case the condition is similar to that obtained previously [12]. Finally, when $P>P_c$ there are two equilibrium points, one of them (v_{01}), which is unstable and the other one (v_{02}), which is stable. Examples of how the potential looks in these cases are plotted in Fig. 2. Since $\dot{v}=0$ all the initial energy of the effective particle is potential energy. This means that collapse can be avoided only when $P>P_c$ *and* the initial width is larger than v_{01} but smaller than a second threshold v_{03} such that $V(v_{03})=V(v_{01})$. In the region of widths given by $v_{03}>v>v_{01}$ the behavior again should be periodic motion around the equilibrium point. This implies that not only collapse is avoided by satisfying the critical condition, but also that the initial condition is important. It is then possible to find the region in the v_0-P plane that leads to collapse behavior. To do so, we have to solve Eq. (17) to find the unstable equilibrium v_{01} and the point v_{03} satisfying $V(v_{01})=V(v_{03})$. The collapsing solutions are those starting with $v<v_{01}$ or $v>v_{03}$. This can be done numerically, and the result is shown in Fig. 3. The meaning of the figure is that if the initial state falls into the shaded region then collapse is avoided. This prediction could be easily checked experimentally by exciting the condensate, once it is in equilibrium, in such a way that the total energy becomes larger than that at $V(v_{01})$. In that case, although Eq. (22) will be satisfied, collapse will occur.

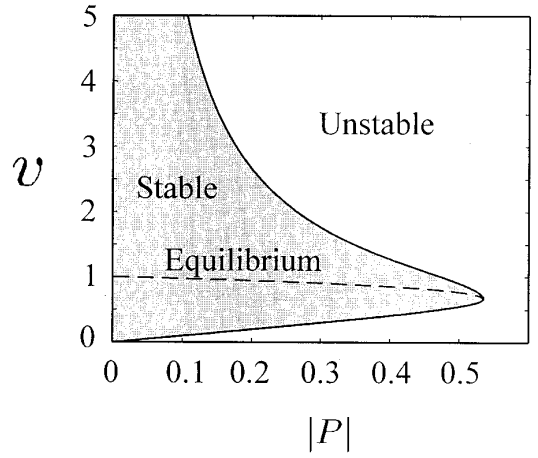

FIG. 3. Conditions for collapse as a function of the initial width v_0 and P values.

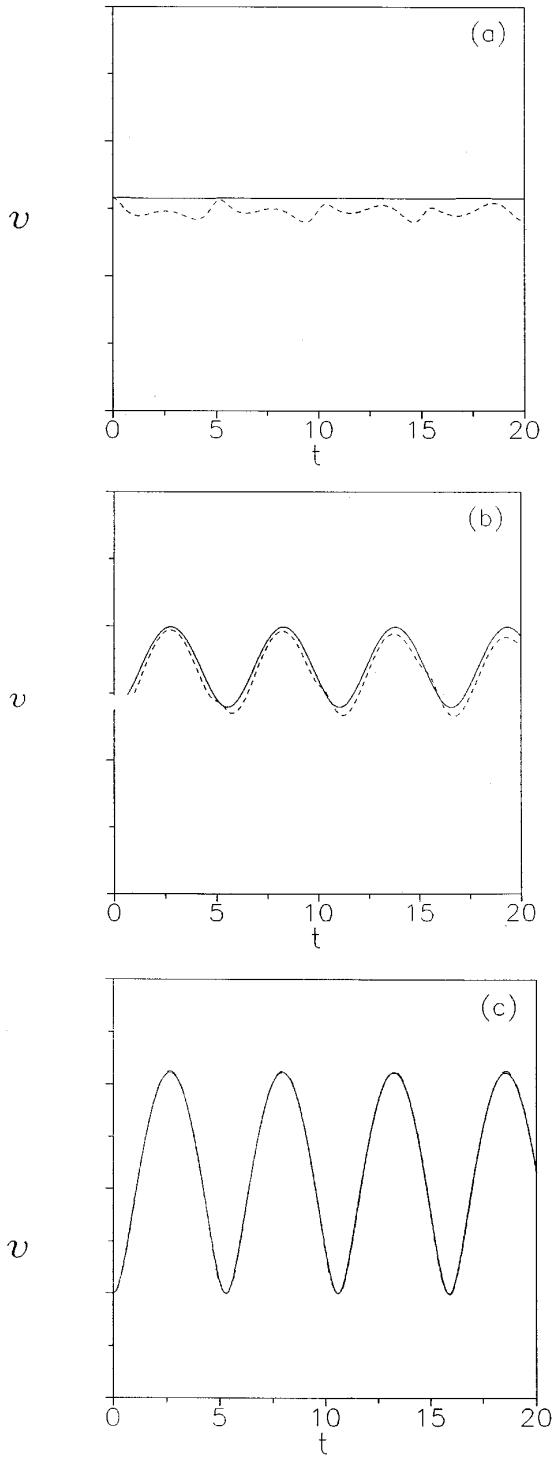

FIG. 4. Evolution of the condensate width in the radially symmetric and negative scattering length case. The dashed curve corresponds to the numerical solution of Eq. (1) and the continuous one to the numerical solution of Eq. (14). (a) $P=0.141$, $v_0=1.032$, (b) $P=0.071$, $v_0=1.30$, (c) $P=0.002$, $v_0=0.802$.

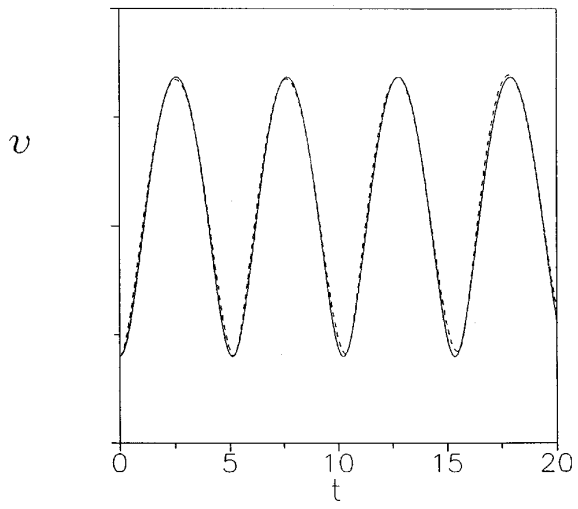

FIG. 5. Evolution of the condensate width in the radially symmetric and negative scattering length case. The dashed curve corresponds to the numerical solution of Eq. (1) and the continuous one to the numerical solution of Eq. (14). Parameter values: $P=0.071$, $v_0=1.30$.

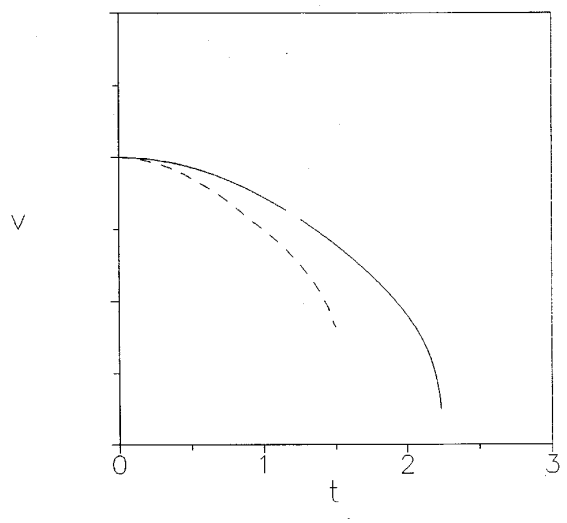

FIG. 6. Evolution of the condensate width in the radially symmetric and negative scattering length cases. The dashed curve corresponds to the numerical solution of Eq. (1) and the continuous one to the numerical solution of Eq. (14). Parameter values: $P=0.6>P_c$, $v_0=1.30$.

D. Numerical simulations

To validate the predictions of the variational method we have performed numerical simulations of Eq. (1) using a highly efficient linearly implicit finite difference conservative numerical scheme [27]. In Fig. 4(a) we see the solution for $P=0.14, v_0=1.032$, which corresponds to the stable equilibrium point of Eq. (14). The wave packet performs some small oscillations around this point, but essentially moves very near to the equilibrium point. When the initial width is increased we see larger amplitude oscillations that are very well represented by the approximate solutions coming from Eq. (14) [Figs. 4(b), 4(c)]. The same good agreement in the dynamics is found for negative scattering length, as can be seen in Fig. 5. Also when the initial width is small enough so that there is collapse, the qualitative behavior is the same (i.e., exact and variational results predict collapse), but the precise form of the collapsing width is somewhat different (Fig. 6). This happens because the self-similar collapsing profile is clearly non-Gaussian. Additionally we see from Fig. 6 that collapse happens with finite width [the numerical solution of Eq. (1) blows up while its width is still finite, which is a well-known fact in mathematical physics [21,34]].

IV. NONSYMMETRIC CASES

A. Discussion

When two of the trap frequencies are equal ($\lambda_x=\lambda_y=1\neq\lambda_z$), as is the case in present experimental systems, and assuming that the oscillations of the condensate keep this symmetry, we get the following evolution equations for the condensate widths

$$\frac{d^2v}{d\tau^2}+v=\frac{1}{v^3}+\frac{P}{v^3v_z}, \tag{23a}$$

$$\frac{d^2v_z}{d\tau^2}+\lambda_z^2v_z=\frac{1}{v_z^3}+\frac{P}{v_z^2v^2}. \tag{23b}$$

The dynamics implied by Eqs. (23a) and (23b) is much richer than that contained in Eq. (14) because of the higher dimensionality of the problem. The equilibrium points are now defined by the equations

$$v_{0z}v_0^4=v_{0z}+P, \tag{24a}$$

$$\lambda_z^2v_{0z}^4=1+Pv_{0z}/v_0^2. \tag{24b}$$

The frequencies of the oscillation around this equilibrium positions are given by

$$\nu_a=2\nu\sqrt{1-2P_{4,1}}, \tag{25a}$$

$$\nu_{b,c}=2\nu\left[\frac{1}{2}(1+\lambda_z^2-P_{2,3})\right. \tag{25b}$$

$$\left.\pm\frac{1}{2}\sqrt{(1-\lambda_z^2+P_{2,3})^2-8P_{3,2}}\right]^{1/2}. \tag{25c}$$

B. Positive scattering length

The equilibrium widths, which always correspond to stable equilibrium points, are given by Eqs. (24) and can be easily found using numerical techniques. With this solution, one can derive the frequencies of oscillation around the equilibrium using Eqs. (25). The corresponding results, together with comparison with experiments, can be found in Ref. [18].

In the Thomas-Fermi limit $P\gg1$ one can find analytical solutions for all these equations. In particular, we find

$$v_0=(P\lambda_z)^{1/5},\quad v_{0z}=[P/\lambda_z^4]^{1/5}, \tag{26}$$

and

$$\nu_a=\sqrt{2}\,\nu, \tag{27a}$$

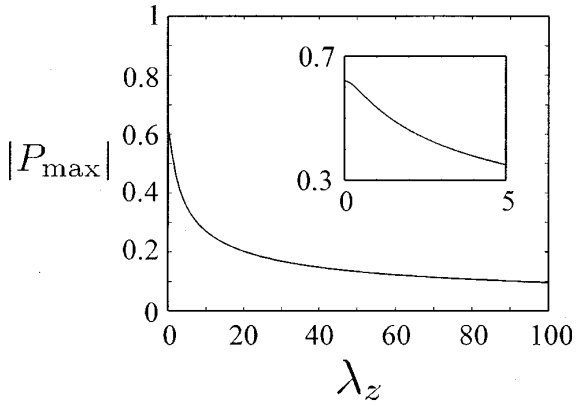

FIG. 7. $P_{\max}$ as a function of λ_z for the case of negative scattering length and cylindrical symmetry.

$$\nu_{b,c}=\frac{\nu}{\sqrt{2}}[4+3\lambda_z^2\pm\sqrt{16+9\lambda_z^4-16\lambda_z^2}]^{1/2}. \quad (27b)$$

These results are in full agreement with those of Stringari [11].

C. Negative scattering length

In Fig. 7 we have plotted the maximum $|P|$ as a function of λ_z such that stable equilibrium points exist. For $\lambda_z=0$ we have

$$|P_{\max}|=\sqrt{\frac{2}{3\sqrt{3}}}=0.6204, \quad (28)$$

whereas for $\lambda_z\gg 1$ it behaves as $|P_{\max}|\simeq 1/\sqrt{\lambda_z}$. This means that for a given scattering length, one can have more particles in the condensate before a collapse takes place if it is cigar shaped ($\lambda_z\ll 1$), rather than coin shaped ($\lambda_z\gg 1$). This is due to the fact that the cigar-shaped condensate is closer to a one-dimensional distribution, for which collapse does not exist, whereas the coin-shaped one is closer to a two-dimensional condensate, where collapse is possible. In Fig. 8 we have plotted the equilibrium widths as a function of $|P|$ for several values of λ_z.

A remarkable feature of this analysis is that even if one releases the trap along the z direction (λ_z), a stable solution exists. This stable object is analogous to the well-known one-dimensional soliton, which appears in the optical fiber context. Let us analyze this solution in more detail. In this case, taking $\lambda_z=0$, Eq. (24) becomes

$$v_0=\frac{|P|}{v_0^3}-\frac{1}{v_0^3 v_{0z}}, \quad (29a)$$

$$|P|v_{z0}=v_0^2, \quad (29b)$$

which gives the following polynomial equation:

$$v_0^6=v_0^2-|P|^2. \quad (30)$$

This equation can have either no or two positive real solutions. In the latter case it is easy to check that one of them

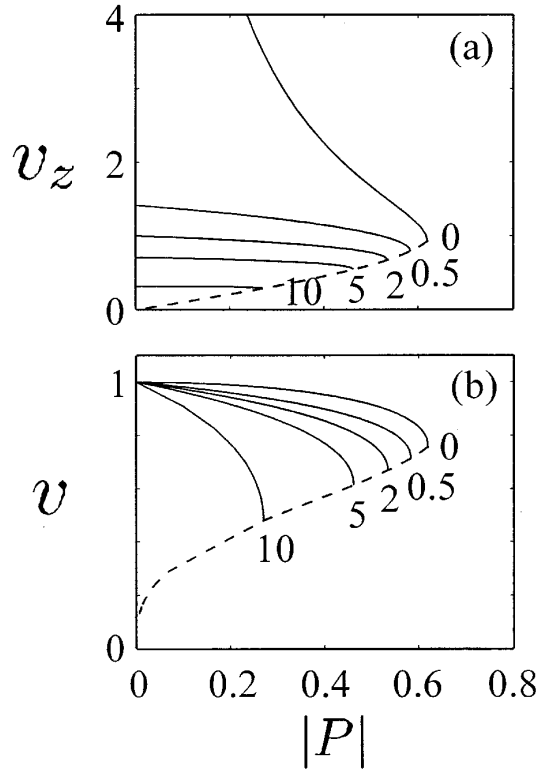

FIG. 8. v_z (a) and v (b) as a function of $|P|$ for several values of λ_z that are indicated on the figure, for the case of negative scattering length and cylindrical symmetry.

corresponds to an stable equilibrium point and the other one to a unstable equilibrium point. What are the implications of this fact? Since we have a stable v_0 point (with a corresponding v_{0z}) we find that it is possible to eliminate one of the trap frequencies and then we could still have a compact object. This is possible due to the attractive self-interaction of the Bose-Einstein gas, which in this case compensates the dispersion provided by the kinetic energy. In fact, there is a simple physical interpretation of this fact that implies that in the free direction the solution is effectively one dimensional and then behaves like a soliton of the one-dimensional NLSE.

Since the solution behaves in a solitonlike manner this opens the door to control its motion by choosing the parameters (e.g., the initial width) to be the one corresponding to this ''compact'' solution and then applying an external potential in the z direction. By the Ehrenfest theorem, the center of mass of the solution will respond to that potential as a particle. This may be useful to guide the motion of the condensate.

We emphasize that for $P>-0.6204$ there is a stable solution. However, if the initial conditions $v(0)$ and $v_z(0)$ are not appropriate (i.e., lie outside the stability region), collapse will occur. In Fig. 9 we have plotted the stability regions for different values of P in the v-v_z plane.

V. CONCLUSIONS

By means of a variational model, analytical expressions for the existence, stability, and evolution of BEC atom clouds have been calculated.

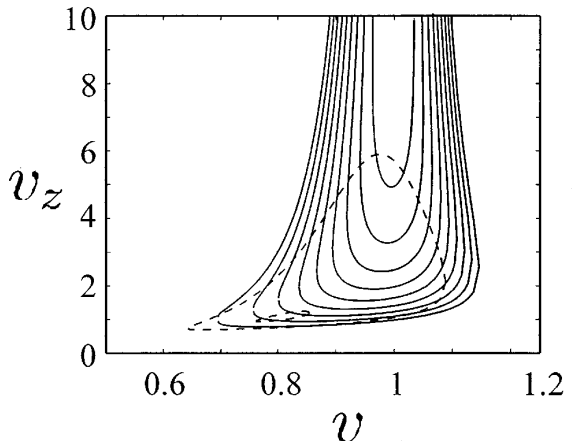

FIG. 9. Stability region for $\lambda_z=0$ and for different values of P ranging from -0.1 to $P_{\max}+0.01$.

The variational method provides a very simple physical picture of the behavior of the condensate: the center of the cloud and its width evolve like particles governed by classical potentials, the initial slope and curvature playing respectively the role of initial speeds of the particles. The evolution equations for the width, which are ordinary differential equations, can be obtained and solved numerically, avoiding complicated numerical simulations of the full $3+1$ problem. We have checked that this approach provides faithful results for the evolution of the width by comparison with numerical simulations of the NLS (GP) in the radial symmetry case. Also some results concerning collapse have been found. The most interesting prediction in this sense is that the initial width of the condensate plays an important role in the collapse dynamics, i.e., if the number of particles is below the collapse limit but the initial width is small enough collapse will take place. Finally, we have predicted the existence of stable trapped solutions, with finite width in the case in which the trap is relaxed along one direction.

The formalism has been successfully applied to the explanation of several experimental results [18]. We believe that the analytical techniques presented in this paper are a useful tool in the analysis of Bose-Einstein condensate dynamics, provide a guide to predict and analyze a whole variety of experimental situations, including the effect of core-core interactions, and can be extended to describe interaction with radiation, losses effects, condensate expansion, etc.

ACKNOWLEDGMENTS

V.M.P-G., H.M., and M.L. acknowledge the hospitality of the Institut für Theoretische Physik, Universität Innsbruck, where part of this work was done. This work was supported in part by the Austrian Science Foundation and by the Spanish Ministry of Education and Culture under Grant No. PB95-0389.

[1] S. N. Bose, Z. Phys. **26**, 178 (1924).
[2] A. Einstein, Sitzungsber. K. Preuss. Akad. Wiss. **1924**, 261 (1924).
[3] E. L. Raab, M. Prentiss, A. Cable, S. Chu, and D. E. Pritchard, Phys. Rev. Lett. **59**, 2631 (1987).
[4] For a review see W. Ketterle and N. J. van Druten, in *Advances of Atomic, Molecular and Optical Physics*, edited by B. Bederson and H. Walther (Academic Press, New York, in press).
[5] M. H. Anderson, J. R. Ensher, M. R. Matthews, C. E. Wieman, and E. A. Cornell, Science **269**, 198 (1995).
[6] K. B. Davis, M.-O. Mewes, M. R. Andrews, N. J. van Druten, D. S. Durfee, D. M. Kurn, and W. Ketterle, Phys. Rev. Lett. **75**, 3969 (1995).
[7] C. C. Bradley, C. A. Sackett, J. J. Tollett, and R. G. Hulet, Phys. Rev. Lett. **75**, 1687 (1995).
[8] M.-O. Mewes *et al.*, Phys. Rev. Lett. **77**, 416 (1996); **77**, 988 (1996); D. S. Jin *et al.*, *ibid.* **77**, 420 (1996).
[9] A. Griffin, Phys. Rev. B **53**, 9341 (1996).
[10] M. Edwards, R. J. Dodd, C. W. Clark, P. A. Ruprecht, and K. Burnett, Phys. Rev. A **53**, R1950 (1996); R. J. Dodd, Mark Edwards, C. J. Williams, C. W. Clark, M. J. Holland, P. A. Ruprecht, and K. Burnett, *ibid.* **54**, 661 (1996); P. A. Ruprecht, Mark Edwards, K. Burnett, and Charles W. Clark, *ibid.* **54**, 4178 (1996); M. Edwards, P. A. Ruprecht, K. Burnett, R. J. Dodd, and Charles W. Clark, Phys. Rev. Lett. **77**, 1671 (1996).
[11] S. Stringari, Phys. Rev. Lett. **77**, 2360 (1996); F. Dalfovo, L. Pitaevskii, and S. Stringari, Phys. Rev. A **54**, 4213 (1996).
[12] G. Baym and C. J. Pethick, Phys. Rev. Lett. **76**, 6 (1996).
[13] B. D. Esry, Phys. Rev. A **55**, 1147 (1997).
[14] L. You, W. Hoston, and M. Lewenstein, Phys. Rev. A **55**, R1581 (1997).
[15] M. Holland and J. Cooper, Phys. Rev. A **53**, 1954 (1996).
[16] Yu. Kagan, E. L. Surkov, and G. V. Shlyapnikov, Phys. Rev. A **55**, R18 (1997).
[17] Y. Castin and R. Dum, Phys. Rev. Lett. **77**, 5315 (1996).
[18] V. M. Pérez-García *et al.*, Phys. Rev. Lett. **77**, 5320 (1996).
[19] P. Nozieres and D. Pines, *The Theory of Quantum Liquids*, (Addison-Wesley, Redwood City, 1990), Vol. II.
[20] In this context, ν is used to denote frequency measured in Hz, which in other context is called ω.
[21] *Nonlinear Klein-Gordon and Schrödinger Systems: Theory and Applications*, edited by L. Vázquez, L. Streit and V. M. Pérez-García (World Scientific, Singapore, 1996).
[22] D. Anderson, Phys. Rev. A **27**, 3135 (1983).
[23] H. Michinel, Pure Appl. Opt. **4**, 710 (1995).
[24] V. M. Pérez-García, M. A. Porras, and L. Vázquez, Phys. Lett. A **202**, 176 (1995).
[25] Y. S. Kivshar and B. A. Malomed, Rev. Mod. Phys. **61**, 763 (1989).
[26] M. Delfour, M. Fortin, and P. Payre, J. Comput. Phys. **44**, 277 (1981); T. R. Taha and M. Ablowitz, *ibid.* **55**, 203 (1984); Y. F. Tang, V. M. Pérez-García, and L. Vázquez, Appl. Math. Comput. **82**, 17 (1997); L. Vázquez, Z. Fei, and V. M. Pérez-García Comput. Math. Appl. **32**, 73 (1996).
[27] Z. Fei, V. M. Pérez-García, and L. Vázquez, Appl. Math.

Comput. **71**, 165 (1995); Z. Fei, I. Martín, V. M. Pérez-García, F. Tirado, and L. Vázquez, in *Nonlinear Coherent Structures in Physics and Biology*, Vol. 329 of *NATO Advanced Studies Institute Series B: Physics*, edited by K. H. Spatschek and F. G. Mertens (Plenum, New York, 1994), pp. 287–298.

[28] E. Caglioti, S. Trillo, S. Wabnitz, B. Crosignani, and P. Di Porto, J. Opt. Soc. Am. B **7**, 374 (1990); A. B. Aceves, A. D. Capobianco, B. Costantini, C. De Angelis, and G. F. Nalesso, Opt. Commun. **105**, 341 (1994).

[29] Z. Fei, V. V. Konotop, M. Peyrard, and L. Vázquez, Phys. Rev. E **48**, 548 (1993); A. Sánchez, A. R. Bishop, and F. Domínguez-Adame, Phys. Rev. E **49**, 4603 (1994); K. O. Rasmussen, O. Bang, and P. L. Christiansen, Phys. Lett. A **184**, 241 (1994).

[30] V. V. Konotop and L. Vázquez, *Nonlinear Random Waves* (World Scientific, London, 1994).

[31] A. Ankiewicz, N. N. Akhmediev, G. D. Peng, and P. L. Chu, Opt. Commun. **103**, 410 (1993).

[32] M. Desaix, D. Anderson, and M. Lisak, J. Opt. Soc. Am. B **8**, 2082 (1991).

[33] P. A. Rupecht, M. Edwards, K. Burnett, and C. W. Clark, Phys. Rev. A **54**, 4178 (1996).

[34] N. E. Kosmatov, V. F. Shvets, and V. E. Zaharov, Physica D **52**, 16 (1991).